Low-Energy Charged Particles in Saturn's Magnetosphere: Results from Voyager 1

Abstract. *The low-energy charged particle instrument on Voyager 1 measured low-energy electrons and ions (energies ≥ 26 and ≥ 40 kiloelectron volts, respectively) in Saturn's magnetosphere. The first-order ion anisotropies on the dayside are generally in the corotation direction with the amplitude decreasing with decreasing distance to the planet. The ion pitch-angle distributions generally peak at 90°, whereas the electron distributions tend to have field-aligned bidirectional maxima outside the* L *shell of Rhea. A large decrease in particle fluxes is seen near the* L *shell of Titan, while selective particle absorption (least affecting the lowest energy ions) is observed at the* L *shells of Rhea, Dione, and Tethys. The phase space density of ions with values of the first invariant in the range ~ 300 to 1000 million electron volts per gauss is consistent with a source in the outer magnetosphere. The ion population at higher energies (≳ 200 kiloelectron volts per nucleon) consists primarily of protons, molecular hydrogen, and helium. Spectra of all ion species exhibit an energy cutoff at energies ≳ 2 million electron volts. The proton-to-helium ratio at equal energy per nucleon is larger (up to ~ 5×10^3) than seen in other magnetospheres and is consistent with a local (nonsolar wind) proton source. In contrast to the magnetospheres of Jupiter and Earth, there are no lobe regions essentially devoid of particles in Saturn's nighttime magnetosphere. Electron pitch-angle distributions are generally bidirectional and field-aligned, indicating closed field lines at high latitudes. Ions in this region are generally moving toward Saturn, while in the magnetosheath they exhibit strong antisunward streaming which is inconsistent with purely convective flows. Fluxes of magnetospheric ions downstream from the bow shock are present over distances ≥ 200 Saturn radii from the planet. Novel features identified in the Saturnian magnetosphere include a mantle of low-energy particles extending inward from the dayside magnetopause to ~ 17 Saturn radii, at least two intensity dropouts occurring ~ 11 hours apart in the nighttime magnetosphere, and a pervasive population of energetic molecular hydrogen.*

The primary scientific objectives of the low-energy charged particle (LECP) investigation are to make particle measurements at low energies ($E \gtrsim 26$ keV for electrons and $E \gtrsim 40$ keV for ions) in the Saturnian magnetosphere in order to characterize the composition of the ion population, to determine particle anisotropies, and to investigate possible particle effects associated with Titan, Rhea, Dione, and Tethys. The LECP instrument has two sensors: the low-energy particle telescope (LEPT) and the low-energy magnetospheric particle analyzer (LEMPA), both of which make use of solid-state detectors. The LEPT is primarily a composition instrument capable of identifying major ion species; LEMPA performs basic ion-electron measurements at low and high energies with good particle definition over a large (~ 10^0 to 10^{11} cm^{-2} sec^{-1} sr^{-1}) dynamic range. The LECP instrument has a stepping motor that rotates the sensors in eight steps through 360° in time intervals ranging from 48 to 384 seconds; this provides angular distribution information from the nonspinning Voyager spacecraft. A full description of the LECP has been given elsewhere (*1*, *2*).

Overview. A summary of the intensity profiles of several particle species during Voyager's passage through the magnetosphere is shown in Fig. 1. Figure 1A shows counting rates of selected electron and ion channels from the LECP, and Fig. 1B presents energy spectral indices (assuming power law spectra for both electrons and ions). Dipole L shells (where L is the equatorial crossing distance of the field lines) of Saturnian satellites as well as bow shock and magnetopause locations are indicated. The entire magnetosphere encounter lasted about 4 days. The most striking aspect of the figure is the differences between the profiles, not only for electrons and ions, but for a single species at different energies.

The intensity of low-energy electrons (Fig. 1A, upper curve) increases up to ~ 5×10^4 above interplanetary values, while the intensity of higher energy electrons (Fig. 1A, second curve from the top) increases up to ~ 10^4. At the magnetopause, low-energy electrons increase substantially more in intensity than do higher energy ones, implying a soft electron energy spectrum at this location, as was found by the Pioneer 11 spacecraft (*3*). Just ouside the L shell of Rhea, however, the intensity of low-energy electrons begins to decrease while the more energetic electrons continue to increase in intensity. The spacecraft went through closest approach to Saturn at 41°S, between the two crossings of the L shell of Tethys, and crossed the planet's equatorial plane near the L shell of Dione outbound. The electron intensities begin to increase rapidly before the second crossing of Tethys' L shell, peaking near the equator and the L shell of Dione. As Voyager continued outbound, the electron intensities begin a rapid decrease soon after, but not coincident with, passage through Rhea's L shell; the intensities reach a local minimum of ~ 1 percent of their prior level at ~ 0900 (unless otherwise indicated, hours are in Universal Time) on day 318. An intensity maximum is observed at ~ 1200 on the same day, with a second intensity minimum measured at ~ 2000. The electron intensities return to preencounter levels at a distance of ~ 50 Saturn radii (R_S) on the dawnside of the magnetosphere. These differences in the intensity profiles of the low- and high-energy electrons are particularly evident in the time dependence of the electron spectral exponent shown in the top curve of Fig. 1B.

The intensity profile of the low-energy ions (Fig. 1A, third curve from the top) is substantially different from that of electrons. The ion flux appears to increase slightly before bow shock crossing, but these ions could be of interplanetary origin. After the magnetopause crossing, the measured ion spectrum is soft (large values of γ) (Fig. 1B, lower trace) in the region that includes the orbit of Titan. This state persisted until ~ 0900 on day 317, when both ion spectra became harder. In terms of flux depletions, the satellite sweeping and absorption effects on these ions are not as pronounced as those of the electrons. The ion intensity continues to increase through the L shells of Rhea and Dione inbound and peaks at the orbit of Dione outbound; there is an indication of a small decrease inside the L shell of Tethys at the time of periapsis.

In contrast to the low-energy ions, the higher energy (~ 550 keV) ions (Fig. 1A) show a large decrease inside the Tethys L shell, similar to that displayed by the energetic α particles. All three ion intensity traces show intensity maxima at the outbound crossing of the Saturnian equator, approximately coincident with the second crossing of Dione's L shell. Inside the magnetosphere the intensity increases of the more energetic ions and the α particles are considerably smaller than those observed for the low-energy electrons and ions. Indeed, our higher energy LEMPA ion data (not shown) indicate little evidence inside the magne-

0036-8075/81/0410-0225$01.50/0

tosphere for the presence of ions with energies $\gtrsim 2$ MeV above the preencounter interplanetary background fluxes. Thus, the magnetosphere of Saturn, outside Voyager's closest approach distance of about 3 R_S ($L \sim 4.3$ R_S), appears to be significantly deficient in high-energy ($\gtrsim 2$ MeV) ions when compared even to the magnetosphere of Earth, confirming the suggestion of the Pioneer 11 investigators (*4*) that the energetic ($\gtrsim 2$ MeV) protons they measured within Saturn's magnetosphere were primarily of solar flare origin.

The intensities of both energetic ($\gtrsim 0.2$ MeV per nucleon) ions and α particles show a gradual increase after the outbound magnetopause crossing, suggesting that the steady-state ion fluxes in the magnetosheath are of interplanetary origin. After the bow shock crossing on day 321, the intensity fluctuations in the low-energy ions continue, with little corresponding activity in the low-energy electrons.

The ion spectral exponent (Fig. 1B) oscillates smoothly between 3.5 and ~ 1. These spectral variations frequently appear to be associated with the intensity structures in Fig. 1A.

Anisotropies. The orientation of Voyager 1 during the inbound traverse of Saturn's magnetosphere allowed the LECP stepping motor to rotate the instrument apertures in a scan plane quite close (~ 30°) to the Saturnian equatorial plane. The instrument could measure pitch angles in the range ~ 90° ± (35° to 75°), and this orientation allows the determination of first-order (convective and gradient) anisotropy with reasonable accuracy. During the outbound trajectory, the LECP scan plane was inclined at an angle of ~ 75° (except during spacecraft maneuvers) to the Saturnian equatorial plane, an orientation in which the detectors sample pitch angles of ~ 90° ± 75°. Although overall coverage of pitch angle increased with this orientation, sensitivity to convective (first-order) effects (in the corotation sense) is greatly reduced.

Despite these limitations, the gross anisotropy picture is rather clear. Figure 2A shows the first-order anisotropies of 53- to 85-keV ions during the entire magnetosphere passage projected onto the *xy* and *xz* planes. The *z* axis is the Saturn spin axis and the *xz* plane contains the Saturn-sun vector. The anisotropies are directed in the corotation sense, consistent with convective **E x B** motion inside the magnetopause, with a rather small component along the radius vector away from the planet. The anisotropy amplitude decreases with distance to Saturn, consistent with convective motion. Density gradient effects at these energies are usually quite small (except near sharp boundaries) as judged by the smoothness of the intensity profile. Scan-averaged vectors at the best available time resolution around the Titan *L*-shell crossing (Fig. 2A, inset) show significant fluctuations in angle about the nominal corotation vector. Considering this variability, it would not be surprising if Titan's geometric wake were offset from its nominal location. Such an offset is reported in the magnetic field signature (*5*).

Passage of the spacecraft into the nightside magnetosheath is evident in the large enhancements of the anisotropy amplitude and the "flaring" in direction in the *xz* plane (Fig. 2A). We find that the anisotropies in the magnetosheath fit an exponential in the cosine of the pitch angle $\sim e^{\alpha\mu}$, where $\alpha \gtrsim 1$ and μ is pitch cosine; α can be interpreted as the ratio of the particle-scattering mean free path to the characteristic scale length of the weakening magnetic field (*6*).

Second-order anisotropies were also determined for both ions and electrons over the entire trajectory (*5*). Samples of pitch-angle distributions are shown in Fig. 2B. In general, the ion distributions can be described as pancake-like throughout the magnetosphere (~ 40 keV to ~ 2 MeV), while the electron distributions are approximately bidirectional, aligned with the field outside the *L* shell of Rhea and pancake-like inside it. The electron anisotropies are also

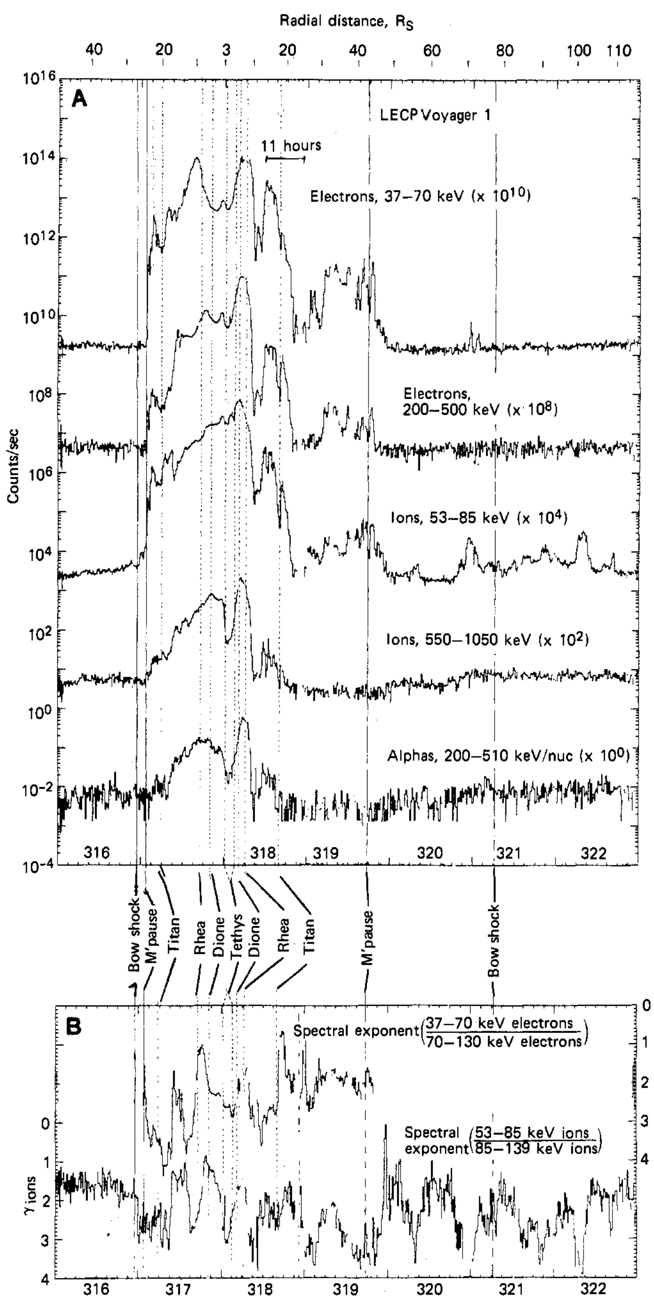

Fig. 1. (A) Summary plot (1-hour averages) of count rates for selected ion and electron channels. The bow shock and magnetopause (*M'pause*) crossings inbound and outbound are marked by solid lines. The calculated *L*-shell crossings of various satellites are shown by dotted lines. (B) Variation of the spectral exponent γ (where dj/dE is proportional to $E^{-\gamma}$, j = particle flux) for ions and electrons. Exponent values are unreliable before day 317 and are uncertain for electrons from day 320 on.

bidirectional in the high-latitude magnetotail, indicating closed field lines. The ion anisotropies in this region are generally directed inward and do not exhibit significant second-order amplitudes.

Energy spectra. As shown in the time dependence of the spectral indices (Fig. 1B), substantial spectral variations in both the electrons and ions were observed throughout the magnetosphere. Figure 3 shows the energy spectra over the available energy ranges of the LEMPA instrument for both electrons and ions for selected time intervals. The spectra of ions (assumed to be protons) shown on the left in Fig. 3A cannot be characterized by a simple power law as they bend over at the lower energies. A change in spectral shape occurs after ~ 0900 on day 317 for energies below ~ 200 keV; the spectra assume forms that can be characterized by two separate power laws above and below that energy. This persists at least through 1200 (see Fig 1B). The highest energy point (2 to 4 MeV) remained consistently at background level ($< 10^{-4}$ cm^{-2} sec^{-1} sr^{-1} keV^{-1}) throughout this interval.

Spectra some 4 hours later (Fig. 3A, right) are definitely bent at the lower energies. These spectra can be fit by an exponential (e^{-E/E_0}, $E_0 \sim 100$ keV) and are somewhat reminiscent of those measured by LEMPA in the high-temperature plasma in the outer magnetosphere of Jupiter. Even throughout this interval, however, the highest energy ion channel (2 to 4 MeV) remained at background.

The electron profiles through ~ 0930 (Fig. 3B, left) can be described by a power law in energy. After this time the spectra become substantially harder, with the largest enhancements observed in the ~ 100 to ~ 400 keV range (and possibly higher). The spectral shape reverts to a power law form by 1100 of the same day. The electron spectra immediately after periapsis, as the spacecraft approached the equatorial plane, are substantially harder and can be described by power laws in energy with slopes of ~ −1 (Fig. 3B, right). Additional data from the LECP instrument (not shown) demonstrate that there are substantial fluxes of electrons > 2 MeV in this time interval. Thus it would appear that in the region sampled by Voyager ($L \geq 4.3$) there is an energy cutoff for protons at ~ 2 MeV, but no similar cutoff for electrons.

Inspection of all ion and electron spectra obtained during the Voyager encounter reveals substantial fluctuations in spectral shape throughout the magnetosphere. Many fluctuations occur in association with crossings of satellite L shells.

Energetic particle pressure and number density. In contrast to the situation at Jupiter (*2*), the ion pressure observed by LEMPA during the Saturn encounter is negligible everywhere in the inner magnetosphere in comparison with the observed magnetic field pressure $B^2/8\pi$ (*5*). The total energy of the observed trapped particle population ($E \gtrsim 40$ keV) is of the order of $\sim 2 \times 10^{21}$ ergs, negligible compared to the total magnetic field energy (about 10^{28} ergs). Hence, no significant ring current effects can be expected from these particles alone. The number density of ions observed by LEMPA also did not contribute importantly to ring current effects. Densities vary from about 3×10^{-4} cm^{-3} at the orbit of Titan inbound to a maximum of about 2×10^{-2} cm^{-3} in the vicinity of the outbound crossing at the L shell of Dione. These number densities are much smaller than those of the low-energy ($\lesssim 8$ keV) plasma reported for the Pioneer 11 flyby (*7*).

Composition of energetic particles. The charged particles in the portion of

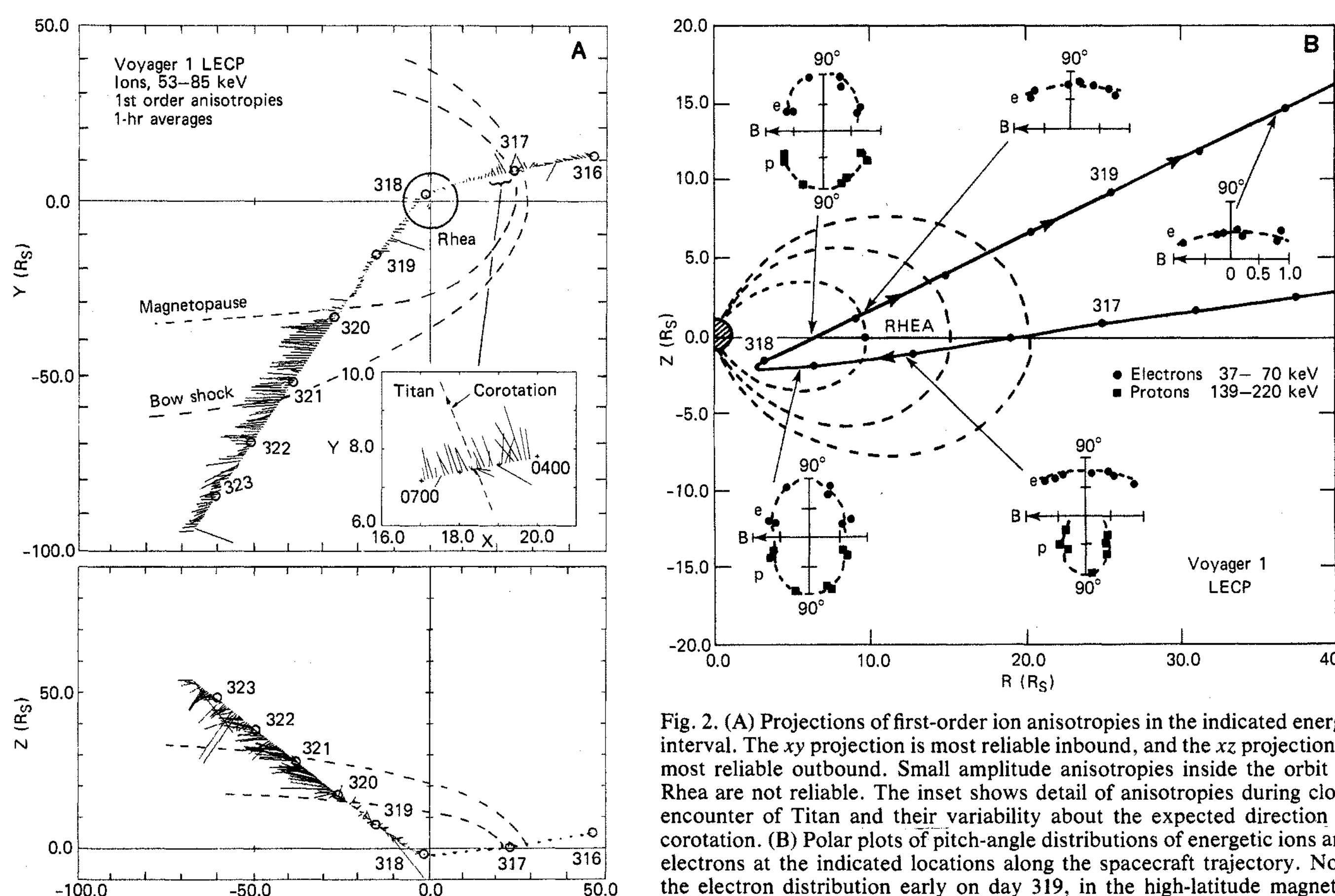

Fig. 2. (A) Projections of first-order ion anisotropies in the indicated energy interval. The *xy* projection is most reliable inbound, and the *xz* projection is most reliable outbound. Small amplitude anisotropies inside the orbit of Rhea are not reliable. The inset shows detail of anisotropies during close encounter of Titan and their variability about the expected direction of corotation. (B) Polar plots of pitch-angle distributions of energetic ions and electrons at the indicated locations along the spacecraft trajectory. Note the electron distribution early on day 319, in the high-latitude magnetosphere. Sample dipole field lines about Saturn are shown by dashed lines. *B*, magnetic field; *e*, electrons; *p*, protons.

Saturn's magnetosphere sampled by Voyager 1 were much less energetic than those in Jupiter's magnetosphere (*8*). Figure 4 presents energy spectra for the three abundant energetic ion species in Saturn's magnetosphere, averaged over a 10-hour period during the inbound pass. The spectra may be described as steep power laws over those rather narrow energy ranges, as was the case throughout the magnetosphere.

The proton and molecular hydrogen spectra are characteristic of magnetospheric particles; however, the helium spectrum has a harder component, arising from a modest interplanetary event that was in progress. The He spectrum taken over a 10-hour period in interplanetary space shortly before Voyager 1 entered the magnetosphere is shown for comparison. It is apparent that above ~ 500 keV per nucleon, the He observed in the outer magnetosphere is largely of interplanetary origin. At smaller radial distances, steeper He spectra, similar in slope to the proton spectra, were observed. No particles of $Z > 2$ were observed at energies $\gtrsim$ 200 keV per nucleon in Saturn's magnetosphere at flux levels higher than those seen outside in the interplanetary event. However, at lower energies (~ 80 to 210 keV per nucleon), an enhancement by a factor of ~ 50 of particles of $Z \geq 6$ was seen, but the species are not resolvable.

The steepness of the H_2 spectrum indicates that the LEPT instrument just caught the extreme tail of the H_2 energy distribution. In fact, no enhanced ion fluxes were seen for any species at total kinetic energies $\gtrsim$ 2 MeV.

The inset to Fig. 4 shows a mass histogram displaying well-resolved peaks at H_2 and He^4 as well as the large peak for protons. The complete absence of H_3 molecules in this energy range is a contrast to their relatively high abundance at Jupiter (*9*).

When abundance comparisons are made at equal energy per nucleon, protons are by far the dominant species. For the period shown in Fig. 4, the proton-to-helium ratio is ~ 1500 at 700 keV per nucleon, which is a lower limit because of the interplanetary He component. For other periods the ratio of H to He is as high as ~ 4400, which is larger than observed in the magnetospheres of either Earth or Jupiter. Preliminary estimates of the ratio $Z \geq 2$ to $Z \geq 6$ in the range 80 to 210 keV per nucleon are ~ 100 to 700, compared to solar system values of ~ 53 (*10*). Based on the large proton to helium ratio, we suggest that energetic protons in the magnetosphere of Saturn must be accelerated from plasma of internal (nonsolar wind) origin. However, the energy spectra are very steep, and if it turns out to be more appropriate to evaluate ratios at equal energy per charge, as at Jupiter (*8*), or total kinetic energy, the abundance ratios take on markedly smaller values.

With regard to H_2, it could be accelerated from either the Saturnian ionosphere along auroral field lines or from Titan's atmosphere. The H_2 to H ratio is highest in the outer magnetosphere, which is consistent with either source.

Satellite absorption effects. Voyager 1 crossed the magnetic dipole L shells of the satellites Titan, Rhea, Dione, and Tethys (Fig. 1). The LECP instrument detected only one deep, localized particle absorption feature (at the L shell of Rhea, which is not visible on the scale of Fig. 1) similar to those found by the Pioneer 11 energetic particle experiments (*4, 11–13*) on the L shells corresponding to the inner satellites and rings. In addition, small, distinct absorption effects ($\lesssim$ 50 percent) are seen in almost all LEMPA channels at the L shells of Dione and Tethys. The particle intensity decreases with decreasing distance inside the L shells of each of the satellites, indicating the signature of inward transport from a source in the outer magnetosphere.

The most pronounced large-scale electron absorption feature detected by LEMPA occurred in the vicinity of the L shell of Rhea during the inbound trajectory (Fig. 1). A rather smooth decrease of low-energy ($\lesssim$ 100 keV) electron fluxes occurs over a distance of the order of 1 R_S along the spacecraft trajectory, the decrease being as much as a factor of ~ 40 in the lowest energy channel (37 to 70 keV) shown. From a preliminary analysis of this absorption feature we can estimate that the mean inward drift speed of the electrons is ~ 20 m/sec, with a corresponding radial diffusion coefficient ~ 4×10^{-8} $R_S{}^2$/sec. Protons were not strongly affected by absorption at Rhea, as would be expected with a diffusion coefficient of this order, and there is only a small effect on the more energetic electrons (0.2 to 0.5 MeV in Fig. 1). This suggests that these more energetic electrons have a longitudinal drift velocity comparable to the satellite orbital velocity and thus are able to cross the satellite L shell with a very low probability for absorption (*11, 13, 14*).

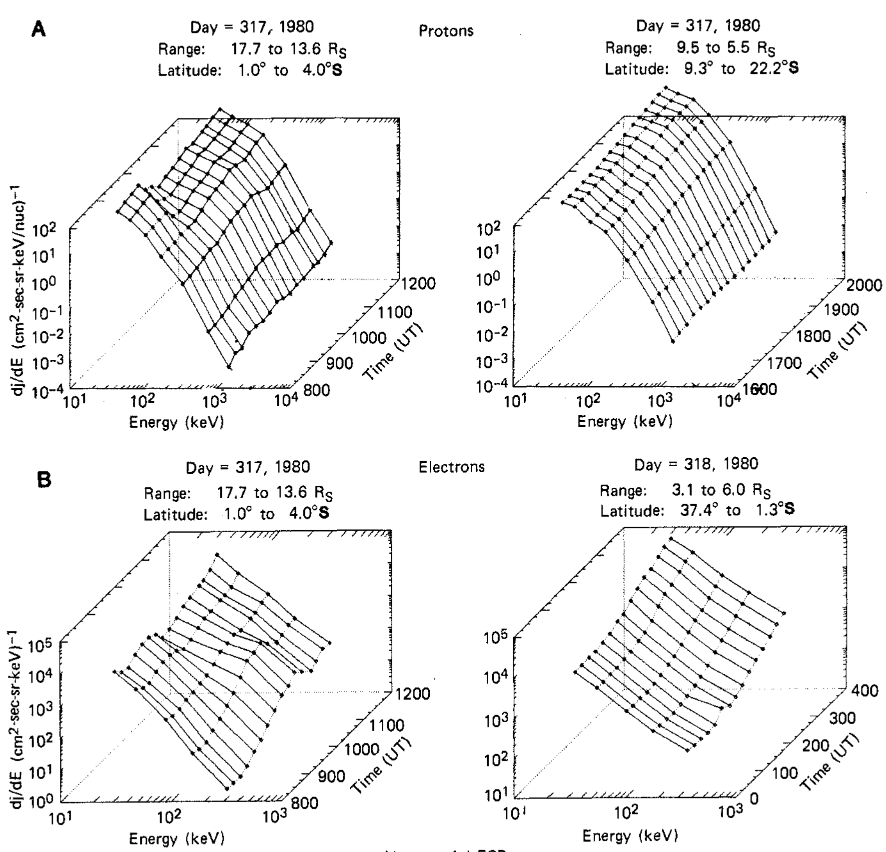

Fig. 3. (A) Time evolution (15-minute averages) of ion spectra. The highest energy point (~ 3 MeV) remains generally at background. Note the substantial evolution in the shape of the spectra. (B) Time evolution of electron spectra. In contrast to the ion spectra, the electron spectra can be described well by a power law in energy, except during spectrum evolution (for example, ~ 1000 to 1100, day 317).

Thus the magnetosphere may not be fully corotating with Saturn at Rhea's orbit, since the resonant energy for rigid corotation is somewhat higher (~ 500 to 600 keV).

During the inbound close encounter with Titan the most noticeable feature in the LECP data is the suppression of the first-order anisotropy seen in the low-energy proton channel (53 to 85 keV) during the satellite wake crossing (Fig. 2A). It is not surprising that a clean absorption feature is not observed in the proton data since the gyromagnetic radii of the ions (~ 15,000 km) are very much larger than the spacecraft-satellite distance (~ 4000 km). Further analysis has revealed a number of wake-produced shadow cones in the data, and these are being investigated.

Both inbound and outbound, however, there appear to be strong absorption effects in the ions and electrons, and these can be ascribed to Titan's torus (Fig. 1). An interesting feature of the region of the magnetosphere containing the Titan L shell is the relatively dense (~ 10 cm^{-3}) neutral hydrogen torus predicted by McDonough and Brice (*15*) and detected by the ultraviolet spectrometer experiment on Voyager 1 (*16*). The charge-exchange lifetime for the lowest energy LEMPA protons is ~ 10^7 seconds. Ion losses at selected pitch angles, such as seen in the Io torus (*17*), may occur in the Titan torus. The absence of a large local absorption effect, however, implies that these particles must be replenished on this time scale (~ 10^7 seconds).

The particles in the vicinity of Titan can have short lifetimes because of the dynamics of the Saturnian magnetosphere. Even small increases of the solar wind pressure on the magnetosphere can push the magnetopause inside the orbit of the moon, as was observed during the Pioneer 11 encounter. In such an event, some of the trapped particles would be lost, and the torus atoms would be dispersed by the solar wind after their ionization. Indeed, the changes observed in the ion and electron spectral indices at ~ 0900 on day 317 (Fig. 1) may be evidence of previous magnetospheric activity that produced changes in the particle populations.

Nightside intensity structure. The intensity profiles of Fig. 1 do not display the symmetry expected in a magnetosphere where the magnetic axis is aligned with the planetary rotation axis (*18*). The abrupt decrease in intensity observed in the nightside magnetosphere at ~ 0700 on day 318 might be explained in terms of the rapid increase in distance of Voyager from the equatorial plane and the presumed plasma sheet, that is, the spacecraft's entry into a lobe-like region devoid of energetic particles as found at Earth and Jupiter. However, as Voyager traveled to even greater distances from the equatorial plane, the particle intensities recover by ~ 1100 and then undergo a second large decrease, reaching another minimum ~ 11 hours later, at ~ 1800. A second intensity recovery begins at ~ 2200, with a possible third decrease at ~ 0900 on day 319 and a third recovery at ~ 1200. After this time, the intensity profile becomes more irregular as Voyager approaches the magnetopause. These ~ 11-hour minima are roughly consistent with a 10-hour 40-minute clock.

Such quasi-periodic intensity variations are also reminiscent of the Jovian nighttime magnetosphere, where they

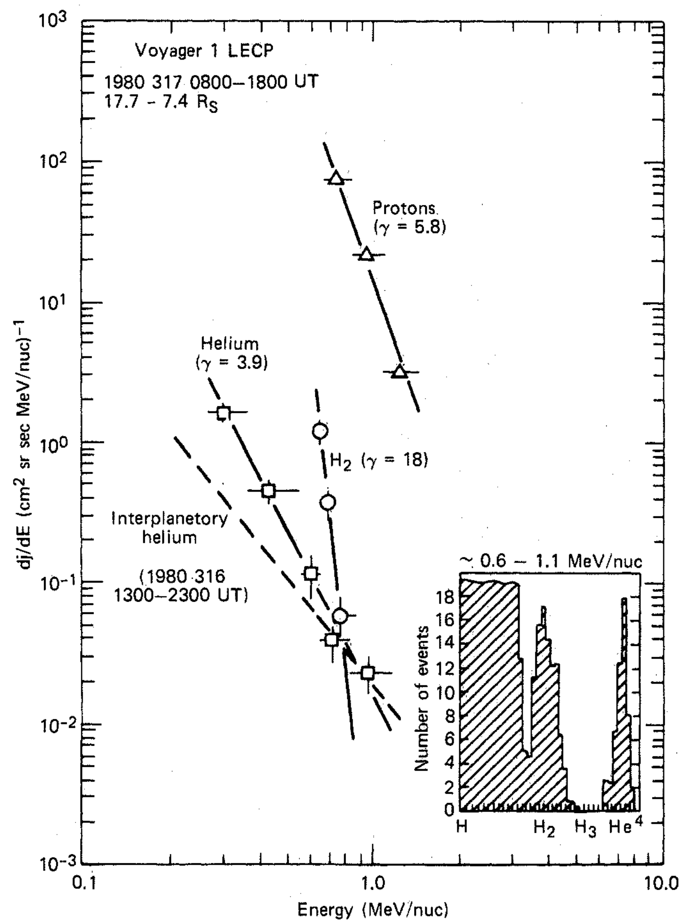

Fig. 4. Pulse-height analyzed spectra for the dominant ion species. Inset shows a mass histogram, revealing strong peaks at H, H_2, and He^4. Note differences in spectral exponents among different components.

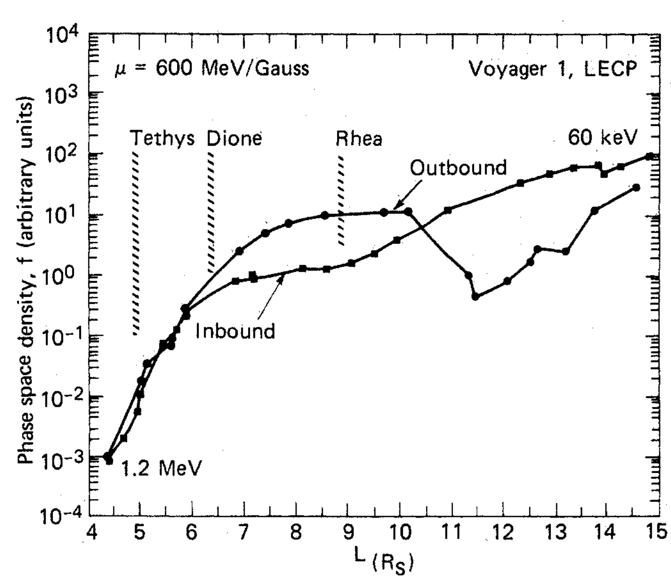

Fig. 5. Phase space densities of ions with a value of the first adiabatic invariant (μ) at 600 MeV per gauss inbound and outbound, computed from observed spectra and angular distributions over the entire range; no assumptions about spectral form were involved.

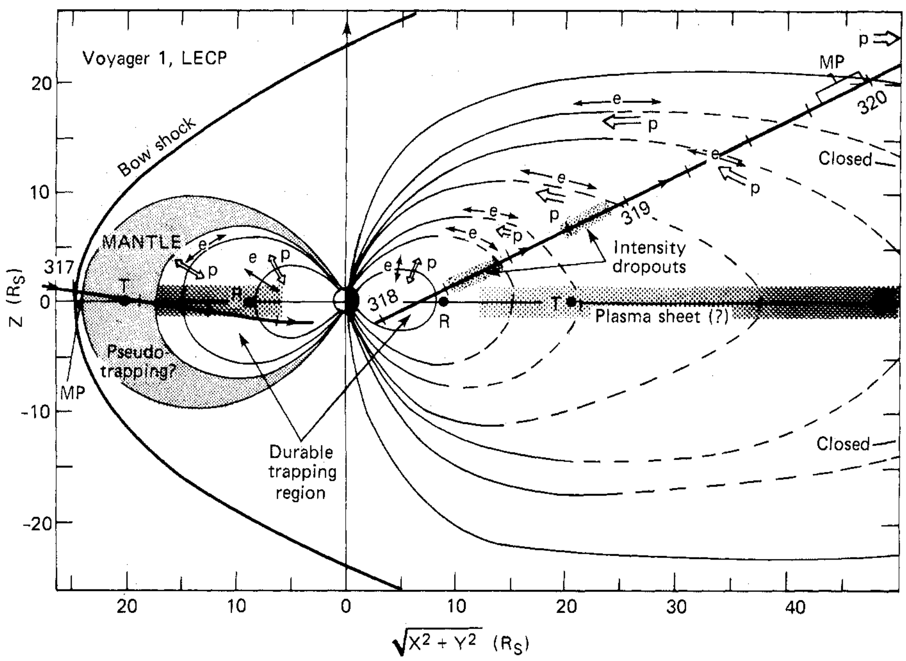

Fig. 6. A schematic representation of Saturn's magnetosphere in the *rz* (trajectory) plane as revealed by the LECP data. Tick marks on the trajectory are at 6-hour intervals from day 318 to 320. Note the Titan-associated mantle region outside ~ 17 R_S, and the presence of closed field lines in the tail lobe region. The phase of the second-order anisotropies relative to the magnetic field (*B*) is shown for both electrons (*e*) and protons (*p*). *R*, Rhea; *T*, Titan; *MP*, magnetopause.

occur because of the tilt of the magnetic dipole of the planet relative to the rotation axis. In the case of Saturn, with only a small dipole tilt (*5*) and the high-latitude spacecraft trajectory, the quasi-periodic intensity variations must have a different origin. We find that the longitude span of the first two minima correspond to a range of ~ 0° to ~ 120° in the coordinate system proposed for radio waves (*19*); the third (uncertain) minimum occurs in the range of ~ 120° to ~ 230°. We note that the ultraviolet spectrometer experiments show an auroral bright region in the longitude range 0° to 120° (*16*).

Although we could speculate on the presence of a magnetic anomaly, as proposed for Jupiter's magnetosphere (*20*), the apparent absence of corresponding intensity features on the dayside may argue against such a hypothesis. The possibility of a Saturnian periodicity in the northern hemisphere may remain just that, due to the limited number of cycles observed before Voyager's exit from the magnetosphere. The absence of obvious periodicities in the dayside intensity profiles might be due to obscuration by satellite absorption effects. It would have been difficult to discern periodicities from the Pioneer 11 data because the particle intensity profiles in the outer magnetosphere were obscured by the presence of solar particles. In addition, the Pioneer 11 trajectory was more or less in the equatorial plane on the dayside, whereas the Voyager intensity dropouts were observed to occur in the northern hemisphere on the nightside.

Phase space ion densities. To investigate the particle source and possible day-night asymmetries, the phase space density (*21*) was computed for the ions over the indicated range of the *L* parameter for both inbound and outbound trajectories (Fig. 5). The observed energy spectra and angular distributions (Figs. 2 and 3) were used and the calculation assumed the nominal magnetic dipole field parameters observed by Pioneer 11 (*18*). The energy coverage of the LECP detector allows calculation of phase space densities over the range ~ 200 to ~ 5 × 10^4 MeV per gauss at ~ 15 R_S, and down to ~ 5 MeV per gauss at ~ 4 R_S.

During the inbound trajectory (Fig. 5) significant changes in slope (indicating localized particle losses) occur at L ~ 11 R_S, ~ 9 R_S, ~ 6.5 R_S, and finally at ~ 5 R_S. These last three changes appear to be associated with the L shells of Rhea, Dione, and Tethys. The general trend is qualitatively similar to that observed by Pioneer 11 (*4, 11*) and suggests that the ion source lies outside 15 R_S. The large ratio of protons to α particles indicates that Titan is a more likely source than the solar wind.

The behavior of phase space density outbound is more complex, however. Although the overall trend is generally similar to the inbound part, intensities in the range L ~ 6 R_S to 10 R_S are enhanced, while at $L \gtrsim 10$ they are depressed. It is possible that significant temporal evolution has taken place, or that the dipole magnetic field model used for the computation of phase space density may not be a good description of the nighttime magnetosphere. The local minimum in phase space density at L ~ 11.5 R_S is most unusual and may be indicative of either particle losses or time variations. This is the same feature discussed above in connection with a possible magnetic anomaly.

Magnetosphere configuration. A schematic compendium of our energetic particle measurements (Fig. 6) highlights several novel features of the Saturnian magnetosphere. This meridional view in the trajectory plane contains the planetary rotation axis, where the inbound cut is near the noon (~ 1300 local time) meridian and the outbound is at ~ 0230 local time. Intensity maxima of electrons and ions relative to the magnetic field are shown by thin and thick arrows, respectively, on ideal dipole field lines at small radial distances, and further out on distended field lines, which have been sketched in as guides. Symmetry between north and south is assumed.

The principal feature on the dayside is the region from the magnetopause to ~ 17 R_S, where the energetic particle spectrum is extremely soft and large convective flows in the corotation direction are observed. This region resembles a plasma mantle and terminates at ~ 17 R_S, where the intensity of higher energy electrons and ions increases rapidly (Fig. 1) and the particle spectra become harder (Fig. 3). It is likely that Saturn's magnetopause is rarely driven inside this distance by the solar wind, and the region inside < 17 R_S is therefore one of durably trapped particles. The magnetopause was located at this distance during the Pioneer 11 encounter, when solar wind pressure was enhanced some eight times over nominal interplanetary values (*22*). Thus, the energetic particle population in this region must be transient.

Notable features on the nightside include the intensity dropouts and the bidirectional electron anisotropies extending all the way to the magnetopause. The first intensity dropout could be understood as the emergence of Voyager 1 from a relatively thin (~ 3 R_S) plasma sheet in the nighttime magnetosphere. The particle intensity, however, recovers at a distance of ~ 4 R_S from the equatorial plane, contrary to what one might have expected by analogy with Earth, where lobe field lines are devoid of particles. It is possible that the dropouts are due to time variations (Saturnian substorm ?), although the occurrence of the second dropout $\sim$ 11 hours after the first makes this less likely. Examination of solar wind activity measured by Voyager 2 upstream from Saturn during this period may help in evaluating this possibility.

As indicated in Fig. 6, the electron pitch angle distribution appears to be field-aligned and bidirectional, suggesting that there exist closed field lines (except in the intensity dropout regions) all the way to the magnetopause at a distance of $\sim 20\ R_S$ above the plane. Ions, on the other hand, show persistent inward flow (toward Saturn) inside the magnetopause with only weak outflow, indicating a source beyond 40 R_S and a probable sink closer to the planet. It is likely that these closed field lines could extend several tens or even hundreds of R_S behind the planet.

In summary, although the magnetic field configuration of Saturn appears relatively simple and dipole-like (*18*), the particle population reveals many striking features in the low-energy spectra, anisotropies, and compositions on both the dayside and nightside, and these features are remarkably different from those of the corresponding populations at Earth and Jupiter.

S. M. KRIMIGIS
Applied Physics Laboratory, Johns Hopkins University, Laurel, Maryland 20810
T. P. ARMSTRONG
Department of Physics, University of Kansas, Lawrence 66044
W. I. AXFORD
Max-Planck Institute for Aeronomy, D-3411 Katlenburg-Lindau 3, West Germany
C. O. BOSTROM
Applied Physics Laboratory, Johns Hopkins University
G. GLOECKLER
Department of Physics and Astronomy, University of Maryland, College Park 20742
E. P. KEATH
Applied Physics Laboratory, Johns Hopkins University
L. J. LANZEROTTI
Bell Laboratories, Murray Hill, New Jersey 07974
J. F. CARBARY
Applied Physics Laboratory, Johns Hopkins University
D. C. HAMILTON
Department of Physics and Astronomy, University of Maryland
E. C. ROELOF
Applied Physics Laboratory, Johns Hopkins University

References and Notes

1. S. M. Krimigis, T. P. Armstrong, W. I. Axford, C. O. Bostrom, C. Y. Fan, G. Gloeckler, L. J. Lanzerotti, *Space Sci Rev.* **21**, 329 (1977).
2. S. M. Krimigis, J. F. Carbary, E. P. Keath, C. O. Bostrom, W. I. Axford, G. Gloeckler, L. J. Lanzerotti, T. P. Armstrong, *J. Geophys. Res.*, in press.
3. J. A. Van Allen, M. F. Thomsen, B. A. Randall, *ibid.* **85**, 5709 (1980).
4. F. B. McDonald, A. W. Schardt, J. H. Trainor, *ibid.*, p. 5813.
5. N. F. Ness *et al.*, *Science* **212**, 211 (1981).
6. E. C. Roelof, *NASA Spec. Publ. SP-199* (1969).
7. L. A. Frank, B. G. Burek, K. L. Ackerson, J. H. Wolfe, J. D. Mihalov, *J. Geophys. Res.* **85**, 5695 (1980).
8. D. C. Hamilton, G. Gloeckler, S. M. Krimigis, L. J. Lanzerotti, *ibid.*, in press.
9. D. C. Hamilton, G. Gloeckler, S. M. Krimigis, C. O. Bostrom, T. P. Armstrong, W. I. Axford, C. Y. Fan, L. J. Lanzerotti, D. M. Hunten, *Geophys. Res. Lett.* **7**, 813 (1980).
10. A. G. W. Cameron, *Space Sci. Rev.* **15**, 121 (1970).
11. J. A. Van Allen, B. A. Randall, M. F. Thomsen, *J. Geophys. Res.* **85**, 5679 (1980).
12. J. A. Simpson, T. S. Bastian, D. L. Chenette, R. B. McKibben, K. R. Pyle, *ibid.*, p. 5731.
13. W. Fillius and C. McIlwain, *ibid.*, p. 5803.
14. A. Mogro-Campero and W. Fillius, *ibid.* **81**, 1289 (1976).
15. T. R. McDonough and N. M. Brice, *Nature (London)* **242**, 513 (1973).
16. A. L. Broadfoot *et al.*, *Science* **212**, 206 (1981).
17. L. J. Lanzerotti, C. G. Maclennan, T. P. Armstrong, S. M. Krimigis, R. P. Lepping, N. F. Ness, *J. Geophys. Res.*, in press.
18. E. J. Smith, L. Davis, Jr., D. E. Jones, P. J. Coleman, Jr., D. S. Colburn, P. Dyal, C. P. Sonett, *ibid.* **85**, 5655 (1980).
19. M. L. Kaiser, M. D. Desch, J. W. Warwick, J. B. Pearce, *Science* **209**, 1238 (1980).
20. A. J. Dessler and V. M. Vasyliunas, *Geophys. Res. Lett.* **6**, 37 (1979).
21. M. Schulz and L. J. Lanzerotti, in *Physics and Chemistry in Space*, J. G. Roederer, Ed. (Springer-Verlag, New York, 1974), vol. 7.
22. J. H. Wolfe, J. D. Mihalov, H. R. Collard, D. D. McKibbin, L. A. Frank, D. S. Intriligator, *Science* **207**, 403 (1980).
23. We thank the Voyager Project Office, JPL, and the Planetary Programs Office, NASA Headquarters, for help and cooperation in carrying out this experiment. We thank D. P. Peletier, S. A. Gary, R. G. King, J. W. Kohl, D. E. Fort, J. T. Mueller, J. H. Crawford, R. E. Thompson, B. A. Northrop, and J. Hook at APL/JHU; E. O. Tums, J. C. Cain, R. T. Cates, R. A. Lundgren, and D. C. Brown of the University of Maryland; C. G. Maclennan of Bell Laboratories; and J. O'Donnell, S. T. Brandon, and M. Paonessa of the University of Kansas for their enthusiasm and long hours that made the LECP experiment a success. The work of E. Franzgrote and D. Griffith of JPL (among many others) was essential to the success of our investigation. We thank N. F. Ness and the MAG team for making their data available before publication, and W. H. Ip for discussions on satellite effects. The LECP program was supported at APL/JHU by NASA under Task I of contract N00024-78-C-5384 between the Johns Hopkins University and the Department of the Navy and by subcontract at the Universities of Kansas and Maryland.

9 February 1981

Energetic Charged Particles in Saturn's Magnetosphere: Voyager 1 Results

Abstract. *Voyager 1 provided the first look at Saturn's magnetotail and magnetosphere during relatively quiet interplanetary conditions. This report discusses the energetic particle populations of the outer magnetosphere of Saturn and absorption features associated with Titan and Rhea, and compares these observations with Pioneer 11 data of a year earlier. The trapped proton fluxes had soft spectra, represented by power laws* $E^{-\gamma}$ *in kinetic energy* E, *with* $\gamma \sim 7$ *in the outer magnetosphere and* $\gamma \sim 9$ *in the magnetotail. Structure associated with the magnetotail was observed as close as 10 Saturn radii* (R_S) *on the outbound trajectory. The proton and electron fluxes in the outer magnetosphere and in the magnetotail were variable and appeared to respond to changes in interplanetary conditions. Protons with energies* $\gtrsim$ *2 million electron volts had free access to the magnetosphere from interplanetary space and were not stably trapped outside* $\sim 7.5\ R_S$.

Voyager 1 traversed Saturn's magnetosphere during relatively quiet interplanetary conditions. The cosmic-ray subsystem (CRS) experiment (*1*) extended the morphology of the outer magnetosphere, as reported by the Pioneer 11 investigators (*2*), to higher latitudes and significantly different interplanetary conditions and provided the first information about the magnetotail at angles $> 90°$ from the Saturn-sun line. A detailed comparison of data from the two missions is important for identifying the processes that shape Saturn's magnetosphere. The Voyager 1 CRS data presented here are restricted to the outer portions of the magnetosphere [$L \gtrsim 7.5$ (*3*)], where the instrument could clearly resolve electrons from protons.

Magnetospheric morphology. Counting rates of protons with energies > 0.43 MeV and 1.8 to 8 MeV are shown in Fig. 1. Also shown are corresponding normalized rates with similar energy thresholds observed by Pioneer 11 (*4*). Voyager 1 entered the magnetosphere three times between 23.7 and 22.9 Saturn radii (R_S) (*5*). Enhancements in the > 0.43-MeV proton flux were observed at each entry. Since no similar flux enhancements were observed during the intervening passages out of the magnetosphere, it is more likely that the enhancements were the result of a transient increase in proton intensity associated with the expansion of the magnetosphere than the result of a permanent layer at the magnetopause. Thus the enhancements observed in the magnetosphere at 22.0 and 21.6 R_S (fourth and fifth peaks) may also have been due to continued radial oscillations of the magnetopause.